JOURNAL OF PROPULSION AND POWER
Vol. 11, No. 1, January–February 1995

# Application of Sweep to Improve the Efficiency of a Transonic Fan Part I: Design

R. J. Neubert,* D. E. Hobbs,† and H. D. Weingold‡
*Pratt and Whitney, United Technologies, East Hartford, Connecticut 06108*

**The concept of aerodynamic sweep has been applied to the design of a highly swept, low-aspect ratio, transonic fan rotor. This design, to be described here, represents the second phase of the Navy Advanced Fan Component Technology program aimed at quantifying the combined performance benefits of low-aspect ratio and of leading-edge aerodynamic sweep on high-pressure ratio transonic fan stages. The first phase included a design and test of a baseline low-aspect ratio unswept fan stage having a design total pressure ratio of 2.2, a tip speed of 1558 ft/s, and relative tip Mach number of 1.6. This baseline fan, designed and tested in 1986–87, achieved its design goals. The design of the swept rotor with the same application requirements was also completed in 1986. The swept design was predicted to be shock free and to improve fan rotor adiabatic efficiency 1.5%. The swept fan performance testing was completed in 1988, and intrablade velocities were measured in 1989.**

## Introduction

AERODYNAMIC sweep has been applied to aircraft wing design since the 1940s to reduce drag at transonic and supersonic flight velocities. It has also been apparent since then that aerodynamic sweep principles might be applicable to turbomachinery blading having supersonic relative Mach number to achieve significant improvements in efficiency. Early attempts were made from the 1940s to 1970s to apply sweep to turbomachinery blading, but were not successful due to the difficulties involved in translating this technology into the confined rotating environment of the gas turbine engine. In this environment, the fan inlet relative Mach number increases from hub to tip due to rotation, both ends of the airfoil are confined, neighboring airfoils are present, and the objective is to achieve a static pressure rise. This technology development culminated in the NASA-sponsored QF-12 fan stage design and test.[1–3] The rotor in this stage had a design supersonic inlet relative tip Mach number of 1.588 and compound swept blading that reduced the effective relative Mach number to subsonic values, ranging from 0.83 at the hub to 0.91 at the mean and tip. The primary goal of the design was to reduce acoustic noise relative to a conventional design through the reduction of shock wave generated multiple pure tones. Unfortunately, the fan rotor failed to achieve the aerodynamic design goals of flow, pressure ratio, and efficiency. Some acoustic tone noise improvements were measured, but again, these changes were below the design expectations. These deficiencies were apparently due to the unexpected radial distribution of the inlet flow induced by the swept rotor. It was also concluded that the potential improvements could be reached with future designs.

The recent development of three-dimensional computational fluid dynamic analysis for transonic turbomachinery blade rows and stages has made the achievement of these envisioned performance improvements feasible in the 1990s. In a recent NASA-sponsored program, these new computational methods were used to explore the application of sweep to moderate pressure ratio, high-aspect ratio fan stages,[4] and in a subsequent Navy-sponsored Navy Advanced Fan Component Technology (NAFCOT) program this new method was used to design a high-pressure ratio, low-aspect ratio fan stage with both an unswept[5] and a swept rotor. This stage includes inlet guide vanes (IGV) and exit stators. The swept design will be described here. The swept rotor performance test program and intrablade laser velocity results are found in Ref. 6, and further details are found in the contract report.[7]

## Discussion

### Amount of Sweep

Fan blades are transonic in the sense that, as a result of their rotational velocity, the inlet blade relative Mach number is usually subsonic at the hub and supersonic at the tip. A simple representation of fan blade section profile total pressure loss coefficient as a function of inlet relative Mach number is illustrated in Fig. 1. At inlet relative Mach number below 0.8, blade section profile losses are primarily due to viscous boundary-layer skin friction, and airfoils can be designed to be free of surface shock waves. Above an inlet relative Mach number of 0.8, losses begin to rise rapidly due to shock losses and shock wave boundary-layer interaction-induced separation losses. As tip speeds are increased, total blade losses rise rapidly since a larger percentage of the blade span is operating at higher Mach number. The application of sweep to transonic blading is intended to reduce the rate at which these losses increase as tip speed is increased.

For the design presented here, the leading edge was swept to a normal component of Mach number 0.8 in an attempt to

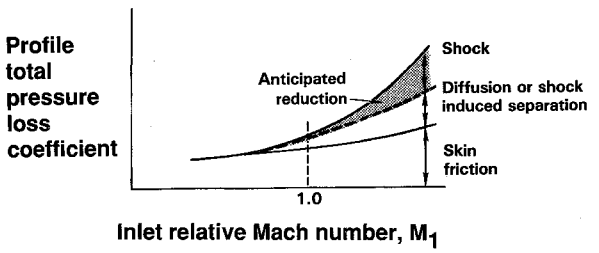


**Fig. 1 Fan blade profile losses vs inlet relative Mach number.**

Received July 7, 1990; presented as Paper 90-1915 at the AIAA SAE/ASME/ASEE 26th Joint Propulsion Conference and Exhibit, Orlando, FL, July 16–18, 1990; revision received July 15, 1992; accepted for publication April 20, 1994. 

*Project Engineer, Compressor Component Group, Engineering Department, M/S 163-17, 400 Main St.

†Project Engineer, Compressor Component Group, Engineering Department, M/S 163-17, 400 Main St. Senior Member AIAA.

‡Senior Research Engineer, Compressor Component Group, Engineering Department, M/S 163-17, 400 Main St. Associate Fellow AIAA.

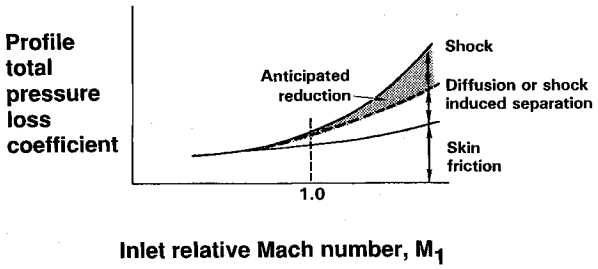


**Fig. 2 Construction of blade leading-edge sweep.**

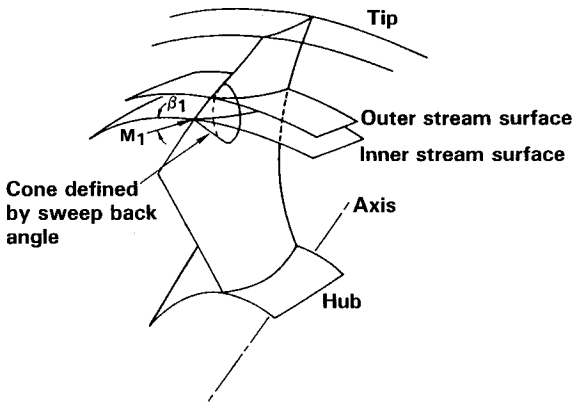


**Fig. 3 Comparison of Mach waves for unswept and swept leading edges.**

completely eliminate shocks and demonstrate the maximum aerodynamic potential of a swept rotor design for this aspect ratio, tip speed, and total pressure ratio. The combined axial and tangential blade leading-edge sweep varies from 60 deg at the tip nearly linearly to 45 deg at the sweep reversal point, at 49% span, and then decreases to 0 deg, at 10% span. This amount of sweep has been estimated to improve fan rotor adiabatic efficiency 1.5%. However, beyond the aerodynamic benefit considerations, there are practical structural, weight, and axial length considerations. Sweeping blades may increase weight, length, and steady stress levels relative to a conventional rotor. It is quite possible that reducing the amount of sweep, with a normal component of Mach number greater than 0.8, will yield a more useful design, considering performance, weight, length, and durability. This optimization problem is currently being examined by Pratt and Whitney, and also, independently by Wennerstrom through a series of tests of conventional and swept rotors designed for the high-through-flow stage.[8]

#### Estimated Efficiency Improvement

The estimated adiabatic efficiency gain of 1.5% for the swept fan rotor relative to the conventional baseline fan is predicated on the swept design eliminating shock waves from the rotor passage. Sweeping the leading edge to a normal Mach number component of 0.8, as shown in Fig. 2, is predicted to permit the accomplishment of this objective by spreading blade pressure disturbances (Mach waves) such that they no longer intersect and reinforce each other (Fig. 3). A heuristic estimate of the loss reduction achievable by eliminating shocks was made by simply reducing the base unswept rotor loss by the loss of a normal shock at the inlet Mach number. No efficiency improvement has been estimated for the reduction of shock related viscous losses, since the predicted extent of boundary-layer separation was not reduced, as discussed below.

Fan efficiency estimates are usually based on a significant base of relevant experimental data. For this radical departure from conventional design, an efficiency estimate based solely on analytical considerations cannot be made with a great deal of confidence. As experimental experience is gained for this type of design, improved efficiency prediction methods will become possible.

**Table 1 Aerodynamic design point**

| | |
|---|---|
| Total pressure ratio | 2.21 |
| Corrected flow, lb/s | 91.5 |
| Adiabatic efficiency, stage, % | 88.1 |
| Polytropic efficiency, stage, % | 89.3 |
| Stall margin, % | 11.3 |
| Specific flow, lb/s/ft$^2$ | 40.4 |
| Corrected tip speed, ft/s | 1558.0 |
| Corrected speed, rpm | 15,870.0 |
| Average $Cx/U$ | 0.43 |
| Inlet hub/tip ratio | 0.41 |
| Rotor aspect ratio | 0.94 |
| Stator aspect ratio | 1.38 |
| Rotor solidity | 1.84 |
| Stator solidity | 1.64 |
| Rotor tip radius, ft | 0.9375 |
| Rotor hub radius, ft | 0.3844 |
| Blade number | 18 |

#### Design Procedure

The design goal of this swept fan rotor was to maintain the aerodynamic design point pressure ratio and flow of the baseline fan rotor while increasing efficiency by sweeping the leading edge to eliminate or reduce shock and shock wave boundary-layer interaction losses. The leading edge was swept such that the normal component of inlet Mach number was subsonic and had a value of 0.8 over the portions of the span where the inlet relative Mach number was greater than 0.8. The airfoil blading design was done fully three dimensionally with an Euler solver, with standard multiple circular arc airfoil sections.

The swept fan design process started with the aerodynamic design point and the basic geometric parameters from the baseline conventional fan rotor defined in Table 1.[5] The leading edge was then swept to give a 0.8 normal component of Mach number (Fig. 2), with an assumed tangential and axial orientation of radially adjacent airfoil sections. The resulting blade was then concurrently analyzed aerodynamically with the three-dimensional Euler solver and structurally with NASTRAN. The results were then used to iterate leading-edge shape, sweep angle, chord length, section thicknesses, section camber, outer flow path contour, and sweep reversal location until a shock-free solution with acceptable radial flow and work distributions and structural characteristics was achieved. Figure 4 shows an overview of this process.

#### Configuration Selection

It is possible to achieve equivalent levels of aerodynamic sweep with a variety of blade configurations, including both simple forward and aft swept airfoils. For this design, in order to minimize relative Mach number, weight, and rotor attachment stress, a compound sweep configuration was chosen where the leading edge is swept forward starting at the hub to a reversal point in the midspan region and then rearward to the tip. This arrangement lowers midspan Mach numbers and allows for balancing the blade center of mass radially over the hub attachment with the minimum hub chord length, lowering attachment stress and weight. Midspan chord was increased to reduce trailing-edge steady stress by straightening the load path along the highly stressed trailing-edge region.

#### Three-Dimensional Euler Solver

The analysis used in the design of the swept fan was a three-dimensional Euler flow solver. The program, by Ni,[9,10] uses a multiple grid scheme along with a second-order integration method to form a fast and accurate solution of the Euler equations. The Euler equations are the inviscid, time-depen-

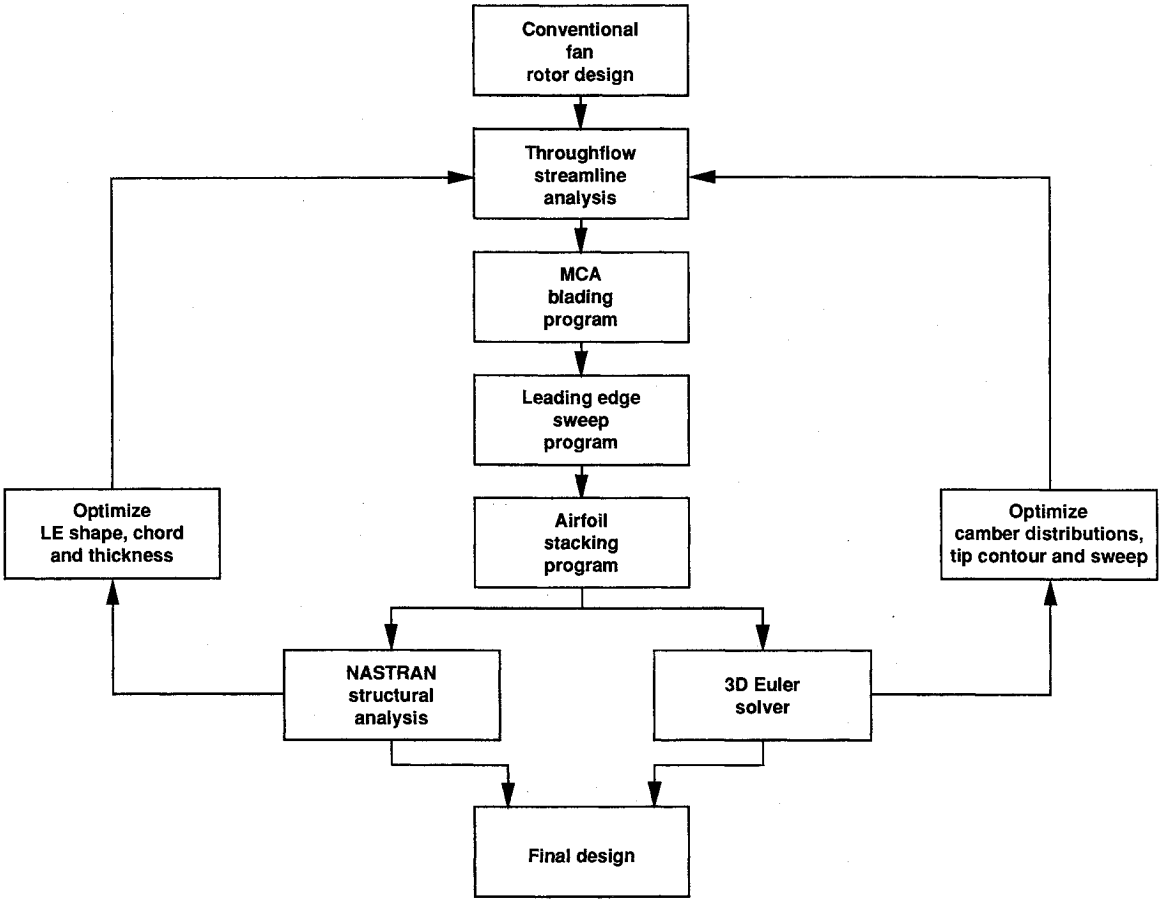


**Fig. 4 Swept fan design procedure.**

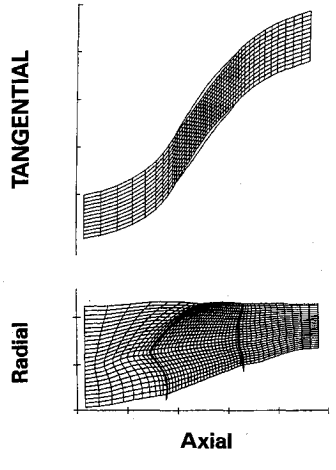


**Fig. 5 H-type mesh for Euler computation.**

dent form of the momentum, continuity, and energy equations. The H-mesh computational grid used for this design, shown in Fig. 5, has 49 axial, 21 spanwise, and 13 blade-to-blade mesh lines.

The approach to the detailed aerodynamic design of swept blading chosen for this design relies on this Euler calculation to evaluate the blade surface pressure distributions in the shockless flowfield. Subsequently, these distributions are used to estimate viscous effects using two-dimensional integral boundary-layer procedures similar to those used in the design of subsonic controlled diffusion airfoils.[11]

Since transonic fan flowfields have strong viscous effects on the inviscid portion of the flowfield, principally due to shock wave boundary-layer interaction, some method must be employed to modify the inviscid Euler analysis to model these effects. This is necessary for the prediction of fan exit flow angle and loss. These models would not have been necessary if a suitable three-dimensional Navier-Stokes analysis had been available for use in the time frame of this design effort. The empirical models employed were a displacement of the blade suction surface and a reduction of the streamwise momentum on both blade surfaces and the endwalls. For unswept fans a large body of data exists that permits calibration of these viscous empirical models. This calibrated procedure can then be used with confidence to design blading that is not too far removed from the calibrating data. However, no such data existed for swept fan designs. Therefore, viscous empirical models were calibrated using the flowfields of unswept fans at subsonic part speed operation. These models were developed only for the design point and assumed to apply over a small range of off-design conditions. Consequently, far off-design conditions, such as stall, could not be analytically investigated during the design.

These empirical calibrations represent the largest risk factor in the swept fan design process, and a second-generation design, which would benefit from the test experience of a first-generation swept fan design, might develop superior performance. The recent development of three-dimensional Navier-Stokes analyses for transonic blading promises substantial improvement to the design methodology for swept blading, eliminating the need for a calibrated Euler analysis.

### Airfoil Section Design and Tip Flowpath Contouring

The airfoil section inlet flow incidence and choke margin were set using static pressure distributions on the suction and pressure sides of the airfoil from the Euler solver. The target distribution was a well-matched subsonic airfoil with as little boundary-layer separation as possible. Exit flow angle devia-

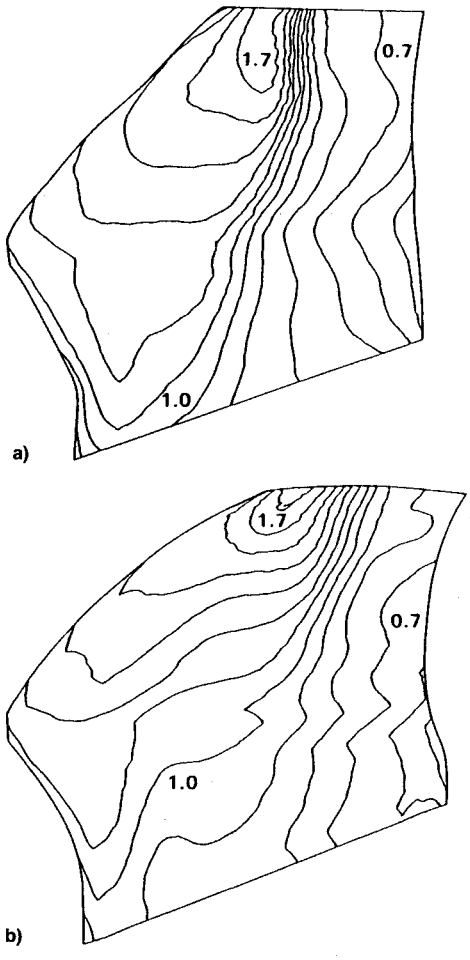


**Fig. 6 Comparison of Mach number contours a) before and b) after camber and tip flow path modifications.**

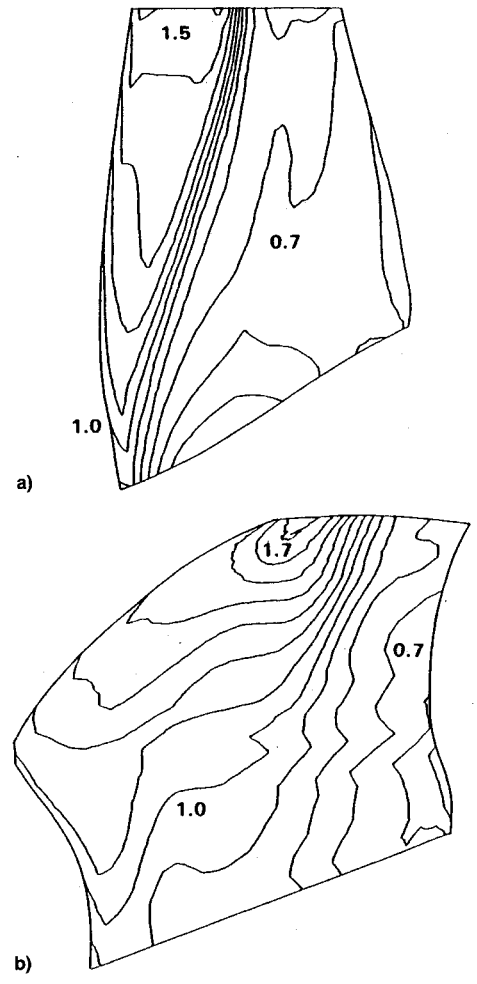


**Fig. 7 Comparison of suction side Mach number contours for the a) swept and b) conventional unswept blades.**

tion levels were set two dimensionally consistent with the closest available fan rotor experience, evaluated at part speed where they were shock-free. Leading-edge sweep causes a chordwise redistribution of work as a function of radius, leading to a radial flow redistribution. This must be compensated for in the design process through adjustment of the radial airfoil stagger and camber distributions. Due to the highly three-dimensional nature of the flow through a swept fan, it was expected that development would be needed to obtain the desired radial distributions of flow and work.

Additional camber optimization was also required in the midspan region, along with outer flow path contouring, to completely eliminate tip shocks. Figure 6 shows a comparison of suction surface Mach number contours, prior to these modifications, with those of the final design.

### Mach Number Contours

Figure 7 shows a computed suction surface Mach contour comparison of the swept rotor relative to the baseline conventional fan. For the baseline rotor, the passage shock appears as a tight concentration of Mach number contours starting near the leading edge at the hub and ending near midchord at the tip. The swept rotor has eliminated this contour line concentration in the hub to midspan region, and significantly spread these concentrations out in the tip region.

The blade-to-blade Mach number contour comparisons along average streamlines are shown for 100, 78, 50, and 18% span in Figs. 8–11. In these figures the airfoils are shown shaded and the Mach number contour levels are 0.1 apart. Note also that the airfoils are scaled to the same chord; where, in fact the swept airfoils were longer. At each span the comparative

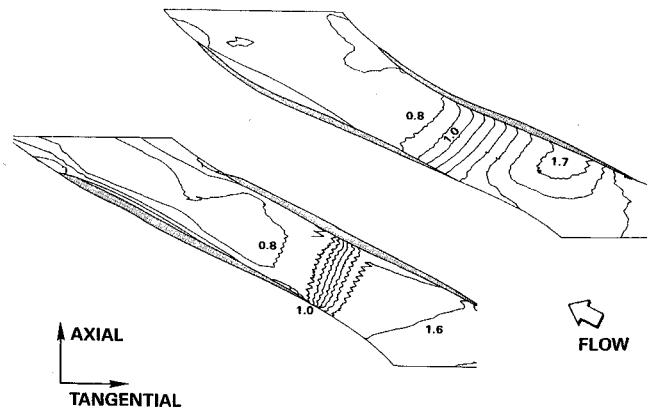


**Fig. 8 Comparison of a) swept and b) conventional unswept blade Mach number contours at 100% span (tip).**

spread of the contour lines confirm that all shocks have been eliminated in the Euler solver solution for the swept blade.

### Boundary-Layer Calculations

As described previously, the computed surface static pressure distributions were used with integral boundary-layer calculations to determine the extent of boundary-layer separation at each span. Since this method is two dimensional, and is not interactive with the Euler solution, the results are currently suspect. However, the method did predict significant amounts of separation, approximately equal to that of the baseline fan. Thus, the static pressure rise, although not predicted to occur through a shock, is still there to separate the

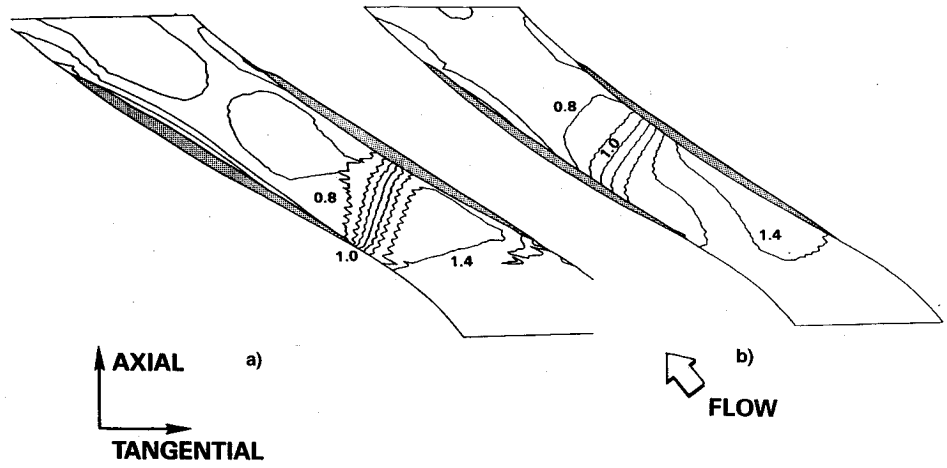


Fig. 9 Comparison of a) swept and b) conventional unswept blade Mach number contours at 78% span.

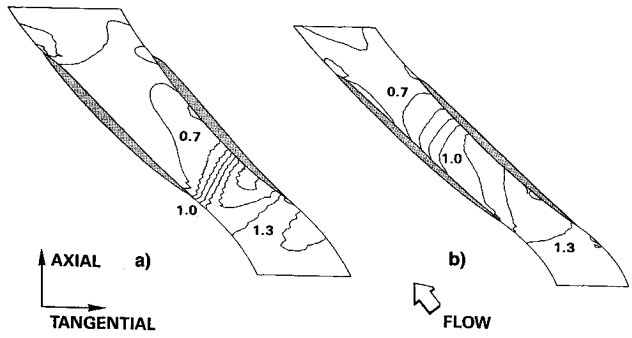


Fig. 10 Comparison of a) conventional unswept and b) swept blade Mach number contours at 50% span.

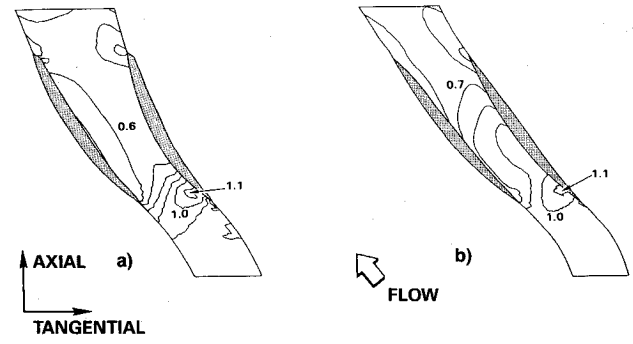


Fig. 11 Comparison of a) conventional unswept and b) swept blade Mach number contours at 18% span.

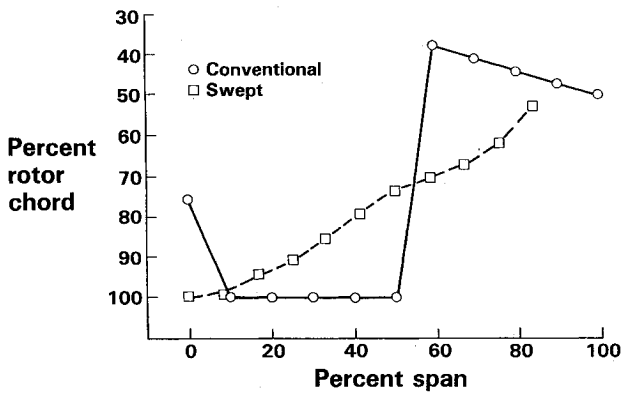


Fig. 12 Comparison of boundary-layer separation locations on the swept and conventional unswept blade suction sides.

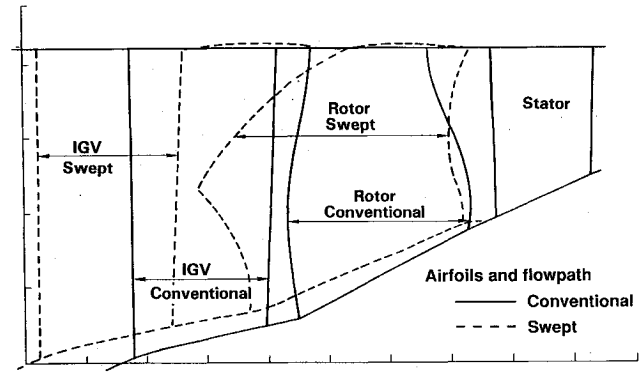


Fig. 13 Comparison of flow paths for swept and conventional unswept fan stage.

boundary layer, where the pressure gradient is high enough. Whether or not these boundary layers subsequently reattach is an open question. Comparison of the results of this analysis for both the swept and conventional blades, shown in Fig. 12, suggests that eliminating shock waves for this design has not reduced, on average, the degree of boundary-layer separation. This result suggests that the contributions of separation to total loss are similar. It should be noted that other swept fans designed for lower total pressure ratio or higher aspect ratio than this application show reductions in boundary-layer separation relative to their unswept counterparts, and have potential for even greater efficiency improvements.

### Flow Path Considerations

As shown in Fig. 13, the swept leading-edge shape and subsequent chord increases required to minimize steady stresses resulted in an increased axial length requirement. In order to maintain inlet guide vane trailing-edge to rotor leading-edge spacing, and rotor trailing-edge to stator leading-edge spacing consistent with stall deflection estimates, the flow path had to be lengthened by about 20%. These flow path changes maintain fan inlet flow area at the baseline fan value.

### Construction of Rotor

The swept rotor design described here has been fabricated for rig testing using an integrally bladed rotor construction, as was the baseline conventional rotor. Figure 14 shows a photograph of these two designs. Another photograph of the swept rotor appears on the cover of Ref. 12. For comparison, the similarly swept NASA QF-12 fan rotor design is also shown in the photograph of Fig. 15.

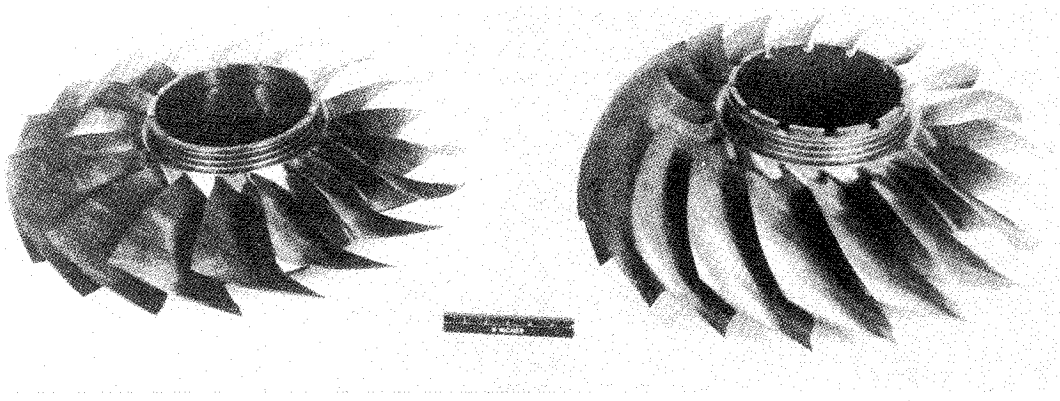


**Fig. 14 Conventional and swept rotors.**

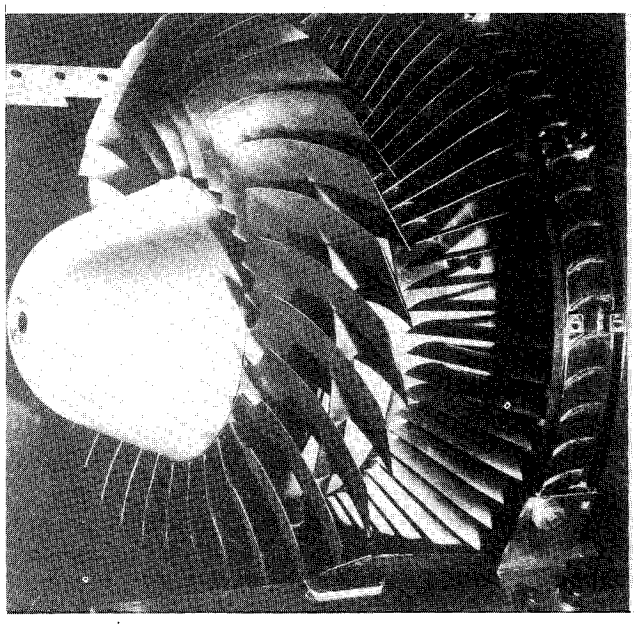

**Fig. 15 Swept NASA QF-12 rotor and fan exit guide vanes.**

## Summary

A design method for swept fans has been described and applied to the design of a high-pressure ratio fan rotor. A comparison of Euler solver flowfields has been made between this swept blade and an unswept blade showing the shock-free character of the swept blade. Finally, boundary-layer separation estimates were compared for the swept and unswept designs, suggesting similar viscous loss for the two designs.

## Acknowledgments

This fan was designed under a NAFCOT project Contract N00140-82-C-H532 with Vern Labosky as the technical monitor. The authors would like to thank the Navy and Pratt and Whitney for permission to publish this article. The photograph of the NASA QF-12 fan was provided by L. J. Bober, Chief of the NASA Lewis Turbomachinery Technology Branch. We would also like to acknowledge the contributions of J. Norton, L. Noryk, and B. Gray to the aerodynamic design; G. Hilbert, B. Chisholm, and D. Houston to the structural design; and R. Ni, J. Bogoian, and K. P. Sarathy to the application of the Euler solver.

## References

[1]Bliss, D. B., Hayden, R. E., Murray, B. S., and Schwaar, P. G., "Design Considerations for a Novel Low Source Noise Transonic Fan Stage," AIAA Paper 76-577, July 1976.

[2]Lucas, J. G., Woodward, R. P., and MacKinnon, M. J., "Acoustic Evaluation of a Novel Swept-Rotor Fan," AIAA Paper 78-1121, July 1978.

[3]Hayden, R. E., Bliss, D. B., Murray, B. S., Chandiramani, K. L., Smullin, J. I., and Schwaar, P. G., "Analysis and Design of a High Speed, Low Noise Aircraft Fan Incorporating Swept Leading Edge Rotor and Stator Blades," Bolt, Beranek, and Newman, Inc., BBN-3332, Cambridge, MA, Feb. 1978; also NASA CR-135092.

[4]Weingold, H. D., Chisholm, B. C., and Dubiel, D. J., "Energy Efficient Engine Hollow Fan Blade Technology-Volume III-Swept Fan Feasibility Study," NASA CR 182223, Aug. 1989.

[5]Creason, T., and Baghdadi, S., "Design and Test of Low Aspect Ratio Fan Stage," AIAA Paper 88-2816, July 1988.

[6]Rabe, D., Hoying, D., and Koff, S., "Application of Sweep to Improve the Efficiency of a Transonic Fan, Part II–Performance and Laser Test Results," AIAA Paper 91-2544, June 1991.

[7]Cheatham, J. G., "Navy Advanced Fan Component Technology (NAFOT) Final Report," Vol. II, Contract N00140-82-C-H532, NAPC-PE-226C, Jan. 1992.

[8]Hah, C., and Wennerstrom, A. J., "Three-Dimensional Flowfields Inside a Transonic Compressor with Swept Blades," American Society of Mechanical Engineers Paper 90-GT-359, June 1990.

[9]Ni, R., "A Multiple-Grid Scheme for Solving the Euler Equations," *AIAA Journal*, Vol. 20, No. 11, 1982, pp. 1565–1571.

[10]Ni, R., and Bogoian, J. C., "Prediction of 3D Multi-Stage Turbine Flow Field Solver Using a Multi-Grid Euler Solver," AIAA Paper 89-0203, Jan. 1989.

[11]Hobbs, D. E., and Weingold, H. D., "Development of Controlled Diffusion Airfoils for Multistage Compressor Applications," *Journal of Engineering for Gas Turbine and Power*, Vol. 106, April 1984, pp. 271–278.

[12]*Aerospace America*, AIAA, Washington, DC, Vol. 28, No. 7, 1990, Cover.